



## **Polarization independent optical injection locking for carrier recovery in optical communication systems**

Downloaded from: <https://research.chalmers.se>, 2025-05-17 09:21 UTC

Citation for the original published paper (version of record):

Jignesh, J., Corcoran, W., Schröder, J. et al (2017). Polarization independent optical injection locking for carrier recovery in optical communication systems. *Optics Express*, 25(18): 21216-21228.  
<http://dx.doi.org/10.1364/OE.25.021216>

N.B. When citing this work, cite the original published paper.



# Polarization independent optical injection locking for carrier recovery in optical communication systems

JOKHAKAR JIGNESH<sup>1,\*</sup>, BILL CORCORAN,<sup>1,2</sup> JOCHEN SCHRÖDER,<sup>3</sup> AND ARTHUR LOWERY<sup>1,2</sup>

<sup>1</sup>*Electro-Photonics Lab., Dept. of Electrical and Computer Systems Engineering, Monash University, Clayton, VIC 3800, Australia*

<sup>2</sup>*Centre of Ultrahigh-bandwidth Devices for Optical Systems (CUDOS), Australia*

<sup>3</sup>*Photonics Lab, Chalmers University of Technology, Göteborg, Sweden*

\*[jignesh.jokhakar@monash.edu](mailto:jignesh.jokhakar@monash.edu)

**Abstract:** An optical injection locking (IL) system that is independent of the incoming signal's polarization is demonstrated for carrier recovery in coherent optical communication systems. A sub-system that enables polarization independence is discussed and experimentally verified. The system is tested over a 20-km test field link using a broad-linewidth laser (40 MHz), and shows the suppression of phase noise when using the carrier recovered by injection locking as the local oscillator.

© 2017 Optical Society of America

**OCIS codes:** (060.1660) Coherent communications; (060.2330) Fiber optics communications; (140.3520) Lasers, injection-locked; (070.1170) Analog optical signal processing.

## References and links

1. A. Umbach, G. Unterborsch, R. P. Braun, and G. Grobkopf, "Stable optical source and high-speed photodetector used for remote fiber-optic 64-GHz mm wave generation," in *Optical Fiber Communication Conf. (OFC '98)*, San Jose, (1998), 260–261.
2. H. K. Sung, T. Jung, D. Tishinin, K. Y. Liou, W. T. Tsang, and M. C. Wu, "Optical injection-locked gain-lever distributed Bragg reflector lasers with enhanced RF performance," in *Proc. of 2004 IEEE Int. Topical Meeting on Microwave Photonics*, Ogunquit (2004), paper MWP.04.
3. H. L. T. Lee, R. J. Ram, O. Kjebon, and R. Schatz, "Bandwidth enhancement and chirp reduction in DBR lasers by strong optical injection," in *Conf. Lasers and Electro-Optics (CLEO 2000)*, Nice (2000), paper CMS4.
4. O. Lidoyne, P. Gallion, C. Chabran, and G. Debarge, "Locking range, phase noise and power spectrum of an injection-locked semiconductor laser," *IEE Proc., J Optoelectron.* **137**(3), 147–154 (1990).
5. S. Uvin, S. Keyvaninia, F. Lelarge, G. Duan, B. Kuyken, and G. Roelkens, "Narrow line width frequency comb source based on an injection-locked III–V-on-silicon mode-locked laser," *Opt. Express* **24**(5), 5277–5286 (2016).
6. M. Lu, H. Park, J. Parker, E. Block, A. Sivananthan, Z. Griffith, L. Johansson, M. Rodwell, and L. Coldren, "A heterodyne optical phase-locked loop for multiple applications," *Optical Fiber Communication Conf. (OFC)*, Anaheim, paper OW3D.1 (2013).
7. L. Naglic, L. Pavlovic, B. Bategelj, and M. Vidmar, "Improved phase detector for electro-optical phase-locked loops," *Electron. Lett.* **44**(12), 758–761 (2008).
8. Z. Liu, D. J. Richardson, and R. Slavik, "Optical injection locking based carrier recovery for coherent signal reception," in *Asia Communications and Photonics Conf. (ACP)*, paper AM31.3, Hongkong (2015).
9. Z. Liu, J. Kim, D. S. Wu, D. J. Richardson, and R. Slavik, "Homodyne OFDM with optical injection locking for carrier recovery," *J. Lightwave Technol.* **33**(1), 34–41 (2015).
10. O. Lidoyne, P. Gallion, and D. Erasme, "Analysis of a homodyne receiver using an injection locked semiconductor laser," *J. Lightwave Technol.* **9**(5), 659–665 (1991).
11. E. Dale, W. Liang, D. Eliyahu, A. A. Savchenkov, V. S. Ilchenko, A. B. Matsko, D. Seidel, and L. Maleki, "On phase noise of self-injection locked semiconductor lasers," in *Proc. SPIE 8960, Laser Resonators, Microresonators, and Beam Control XVI*, 89600X (2014).
12. S. L. I. Olsson, B. Corcoran, C. Lundström, E. Tipsuwannakul, S. Sygletos, A. D. Ellis, Z. Tong, M. Karlsson, and P. A. Andrekson, "Injection locking-based pump recovery for phase-sensitive amplified links," *Opt. Express* **21**(12), 14512–14529 (2013).
13. M. Selmi, Y. Jaouen, and P. Ciblat, "Accurate digital frequency offset estimator for coherent PolMux QAM transmission systems," in *Proc. of European Conf. on Optical Communication (ECOC)*, paper P3.08, Vienna (2009).

14. D. S. Millar and S. J. Savory, "Blind adaptive equalization of polarization-switched QPSK modulation," *Opt. Express* **19**(9), 8533–8538 (2011).
15. M. G. Taylor, "Phase estimation methods for optical coherent detection using digital signal processing," *J. Lightwave Technol.* **27**(7), 901–914 (2009).
16. J. Jokhakar, B. Corcoran, and A. J. Lowery, "Polarization-independent optical injection locking," in *Optical Fiber Communication Conf. (OFC)*, paper Th4I.4, Los Angeles (2017).
17. M. Mazur, A. Lorences-Riesgo, M. Karlsson, and P. A. Andrekson, "10 tb/s self-homodyne 64-qam superchannel transmission with 4% spectral overhead," in *Optical Fiber Communication Conf. (OFC)*, paper Th3F.4, Los Angeles (2017).
18. R. Noé, B. Koch, V. Mirvoda, and D. Sandel, "Endless optical polarization control and PMD compensation," in *Optical Fiber Communication Conf. (OFC)*, paper OThJ1, San Diego (2010).
19. A. Fragkos, A. Bogris, D. Syvridis, and R. Phelan, "Amplitude Limiting Amplifier for Phase Encoded Signals Using Injection Locking in Semiconductor Lasers," *J. Lightwave Technol.* **30**(5), 764–771 (2012).
20. R. Lodenkamper, T. Jung, R. L. Davis, L. J. Lembo, M. C. Wu, and J. C. Brock, "RF performance of optical injection locking," *Proc. SPIE* **3463**, 227–236 (1998).
21. R. A. Shafik, Md. S. Rahman, A. H. M. R. Islam, "On the extended relationships among EVM, BER and SNR as performance metrics," in *Proc. of International Conf. on Electrical and Computer Engineering* (2006), Dhaka, Bangladesh, 408–411.
22. P. Robertson and S. Kaiser, "Analysis of the effects of phase-noise in orthogonal frequency division multiplex (OFDM) systems," in *Proc. of IEEE International Conf. on Communications. (ICC)*, Seattle, WA, (1995), **vol.3** pp. 1652–1657.
23. M. Noroozi, A. Zahedi, and H. Bakhshi, "Compensation of phase noise in OFDM systems using a CPE and channel estimation scheme," in *Proc. of Int. Symp. on Performance Evaluation of Computer and Telecommunication Systems*, Edinburgh (2008), pp. 197–201.
24. D. Chang, F. Yu, Z. Xiao, N. Stojanovic, F. N. Hauske, Y. Cai, C. Xie, L. Li, X. Xu, and Q. Xiong, "LDPC convolutional codes using layered decoding algorithm for high speed coherent optical transmission," in *Proc. of Optical Fiber Communication Conf. (OFC)*, paper OW1H.4, Los Angeles (2012).

## 1. Introduction

Optical injection locking (IL), which forces a 'slave' laser to follow the phase trend of a 'master' injected signal, has found many applications over the past decade. These applications include: all-optical regeneration of signals [1], increasing the linear gain regime of laser [2], bandwidth enhancement of lasers [3], laser linewidth (LW) reduction [4], phase-locked mode generation for a mode-locked laser [5], optical phase-locked loops [6,7] and carrier-recovery in coherent optical systems [8–11].

In coherent optical communication systems, optical carrier recovery mitigates perturbations in the phase-encoded data, caused by the phase noise of the lasers and finite carrier-frequency offsets (CFO) between the transmitter's laser, and the receiver's local oscillator (LO). Demonstrated analog carrier-recovery methods include optical and electro optical phase locked loops (PLLs) [6]. Optical PLLs track the phase of the incoming signals and provide appropriate feedback to the remove the phase offsets [6]. Although PLLs can track both phase offsets and CFO, sub-system complexity has restricted practical implementations in communication systems. Electro-optic phase locked loops have also been proposed [7]. These systems are still relatively complex to implement, and are restricted to CFOs of 100's of MHz and phase noise bandwidths on the order of 1 MHz, by the latency of the electrical components in the feedback. In the digital domain, different signal processing techniques have been used to compensate for CFO and phase noise (e.g [12–15]). The consistent problem faced by analog and digital methods is the amount of phase noise and CFO that can be compensated for, which is either restricted by the device-bandwidths and setup-complexity in analog devices or computational complexity in DSP algorithms. These methods are useful in the best-case scenarios to LWs on the order of 1 MHz and frequency offsets on the order of 1 GHz. In contrast, optical injection locking has been shown to achieve carrier recovery for an offset of tens of GHz [8–11], without introducing latency in signal recovery in addition to providing > 90% phase transfer with optical signal to noise ratios (OSNR) down to 0 dB [12]. Injection locking the receiver-side LO laser by using a residual carrier wave from the incoming signal transfers the phase noise of the signal carrier onto the LO, which enables all-optical recovery of the carrier from coherent reception [8–10].

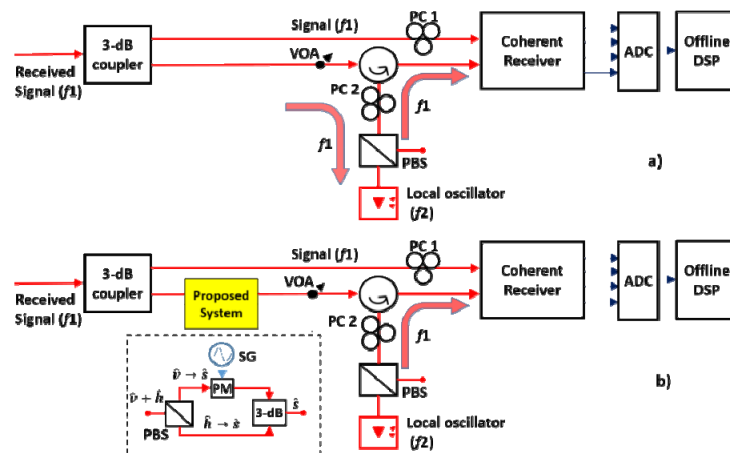


Fig. 1. Receiver system: a) conventional IL setup; b) IL setup with the proposed modifications. VOA: variable optical attenuator; PC: polarization controller; PBS: polarization beam splitter; SG: signal generator; ADC: analog-to-digital converter; PM: phase modulator.

A homodyne setup as shown in Fig. 1(a) is used where the received signal is split using a 3-dB coupler with the signal in one arm fed directly to the coherent receiver and the signal in the other arm injected in the cavity of a local oscillator (LO) laser. If the free-running frequency of the LO laser ( $f_2$ ) and the frequency of the injected signal and laser characteristics, the LO signal locks on to the frequency of the injected signal, essentially removing the effects of phase noise and the CFO [8–11].

To achieve the locked state of the IL, the incoming signal is injected into the cavity of the slave local oscillator laser. This cavity is, however, aligned to a single state of polarization (SOP). As a result, proper locking can be achieved only if the incoming signal's state of polarization is aligned with that of the LO laser cavity and stabilized over the period of operation. In previously demonstrated IL systems, this is achieved by alignment using the polarization controller PC2 and PBS in Fig. 1(a). Although this method works perfectly in a confined lab environment, links in underground ducts are prone to vibrations and pressure variations due to surrounding vehicular motions, human activities and general environmental variations, causing the SOP of the received signal to randomly change over time. As a result, the alignment between the LO lasing polarization and the incoming carrier will drift and may result in loss of locking for sustained polarization fades. To prevent this, the system needs to be constantly monitored and needs to be aligned whenever the SOP of the incoming signal changes, which requires a complex system of polarization monitoring, polarization-state control and a stable feedback loop. As an alternative, in this paper, we propose and demonstrate a polarization-locking module that, when plugged in the IL setup as shown in Fig. 1(b), renders the IL independent of the incoming signal's SOP. This is an extension of the work presented in the OFC 2017 conference [16].

We demonstrate that our system based on an interference mechanism maintains injection lock for any random state of polarization of the injected signal. The proposed polarization-locking module may cause the system to go in to a deep fade due to its interfering mechanism, and eventually result in loss of lock. To prevent this, phase modulation was added to frequently push the system away from the points of deep fades. The consequential amplitude fluctuations, caused by the interfering mechanism and the phase modulations, were considered and shown to be sufficiently suppressed by the IL's amplitude transfer characteristics. Experimental demonstrations in back-to-back setup and over a 20-km field trial showed that the system implementing the proposed module with the injected power as low as  $-25$  dBm performed without  $Q$  penalty, similar to a conventional intradyne system

with a narrow LW (100 kHz) laser. Experiments were also performed with a low-output-power (0.5 dBm), broad-LW (40 MHz) laser at the transmitter, for which the data recovery failed in the intradyne system, but was successfully achieved when using the injection locked system. At this broad linewidth, the blind phase estimation algorithms fail due to cycle slips. Training-based phase estimation could work for this broad linewidth but at the cost of increased overhead. On the other hand, a self-homodyne receiver (with injection locking in our case) aided with blind phase estimation, can perform equally well or better than the training based phase estimation for such broad linewidths [17]. In all the cases, the proposed polarization-locking module was verified to work without  $Q$  penalties or locking bandwidth compared with an injection-locked system without the module. However, the system without the module repetitively lost the lock when tested over the field trial and needed timely realignment of the polarization controllers, which was solved in the system implementing the proposed module.

Section 2 discusses the design and working of the proposed polarization-locking module. Section 3 describes the proof of concept experiments and results. The experiment with an optical OFDM signal in a back-to-back setup is shown in Section 4 where the system with proposed module was verified to work without  $Q$  penalties in spite of fluctuating polarization rotation, phase and amplitude perturbations. Section 5 discusses the broad-LW experiments where the injection locking manages to recover the data when using a broad-LW laser. Section 6 covers the field trial experiment over a 20-km test link. Section 7 concludes the paper with the inferences made from the experimental results.

## 2. Proposed module design and modifications to IL setup

To make the injection locking independent of the incoming signal's SOP, a module was designed that can be plugged in before the IL setup, as shown in Fig. 1(b); the module design is shown in Fig. 2.

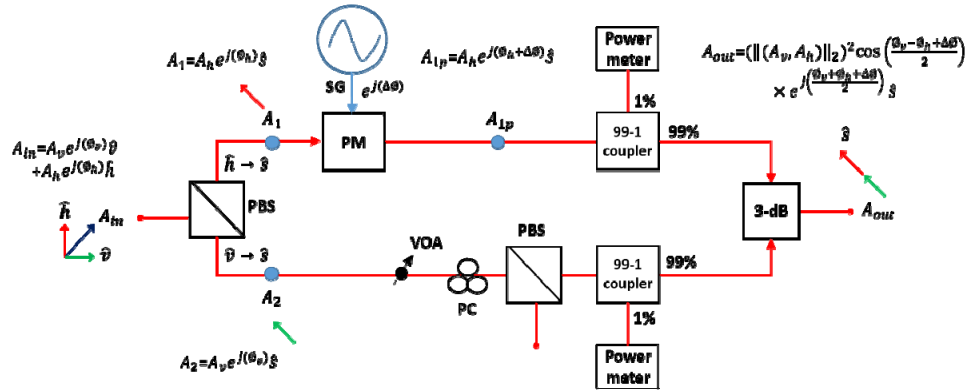


Fig. 2. Proposed polarization-locking module design with working concept.

Consider a signal ( $A_{in}$ ) at the input of the proposed module (left, Fig. 2), which has a random SOP that can be resolved into finite components in the vertical  $\hat{v}$  (red) and horizontal  $\hat{h}$  (green) polarization axes,

$$A_{in} = A_v e^{j\phi_v} \hat{v} + A_h e^{j\phi_h} \hat{h} \quad (1)$$

The PBS in the module separates these components on to the slow axis ( $\hat{s}$ ) of its two output arms (i.e. horizontal component to the top arm in Fig. 2 at Point  $A_1$ , vertical component to the bottom arm at Point  $A_2$ ). Hence both the polarization components are aligned on the slow axis.

$$A_1 = A_h e^{j\phi_h} \hat{s} \text{ and } A_2 = A_v e^{j\phi_v} \hat{s} \quad (2)$$

Conceptually, if we were to then simply combine  $A_1$  (red) and  $A_2$  (green) using a polarization-maintaining 3-dB coupler, we can convert the incoming signal's random SOP in to a constant known state ( $\hat{s}$ ). As a result, despite of the incoming signal having a random SOP, the output of the polarization-locking module will be permanently aligned on a known state of polarization. However, any phase difference between  $A_1$  and  $A_2$  leads to a fade in amplitude if the output of the coupler. When the SOP of the signal is such that the  $\hat{h}$  and  $\hat{v}$  polarization components are opposite phase, interference through the 3-dB coupler will cause destructive interference. If the module is then placed before injection locking, this destructive interference will result in lower injected power, which can result in the LO unlocking for long fades.

To prevent long power fades, a phase modulator was added in one arm of the proposed module as shown in Fig. 2. The phase modulator modulates the incoming optical signal with a low-frequency (400 kHz) sinusoidal signal generated by a signal generator (SG). The frequency of phase modulation is chosen to be higher than the speed of polarization rotations in practical systems, which can be on the order of kHz [18]. This then converts potentially long, uncontrolled power fades into a relatively rapid (400 kHz) amplitude modulation.

In practice, the signal in the upper arm of Fig. 2 is attenuated due to the insertion loss of the phase modulator; this attenuation is balanced in the other arm by a VOA, to ensure equal powers at the two inputs of the 3-dB coupler. Because in our experiment the VOA is not polarization maintaining, and the inputs of the 3-dB coupler need to be aligned to the same fixed polarization, an additional PBS and polarization controller are used, as shown in Fig. 2. This complexity can be reduced by using all polarization maintaining components. Referring back to Fig. 2, the output of the phase modulator can then be represented as

$$A_{1p} = A_h e^{j(\phi_h + \Delta\phi)} \hat{s} \quad (3)$$

where, in our experiments,  $\Delta\phi$  is a 400-kHz sinusoidal phase modulation. When  $A_2$  and  $A_{1p}$  are combined in a polarization-maintaining 3-dB coupler, we get

$$A_{out} = (\| (A_h, A_v) \|_2)^2 \cos\left(\frac{\phi_h - \phi_v + \Delta\phi}{2}\right) e^{j\left(\frac{\phi_h + \phi_v + \Delta\phi}{2}\right)} \hat{s} \quad (4)$$

The equations are derived without considering the losses in the upper of the polarization-locking module. Owing to the cosine term changing with  $\Delta\phi$ , the power out of the 3-dB coupler continuously fluctuates at 400 kHz. These low-frequency intensity fluctuations would be detrimental if passed through to the LO. In order to suppress these intensity fluctuations, we exploit the innate phase and amplitude transfer characteristics of IL systems at low injection ratios ( $< -30$ -dB). Under locked conditions and within the locking range, the IL system transfers phase modulation, replicating phase information. At the same time, the amplitude modulations can be highly suppressed [19,20]. Consequently, the amplitude fluctuations at the output of the 3-dB coupler caused due to the low frequency phase modulation ( $\Delta\phi$ ) on one arm of the module will be suppressed, whereas the required carrier phase information will pass through. The phase modulation,  $\Delta\phi$  also show up in the phase of the output which will get transferred through the IL setup. However, this phase modulation can be compensated for by the phase estimation algorithms running in the DSP, as the frequency (400-kHz) is much lower than the symbol rate. Thus, the fixed SOP can be maintained at the output of the module without losing injection locking.

### 3. Proof of concept

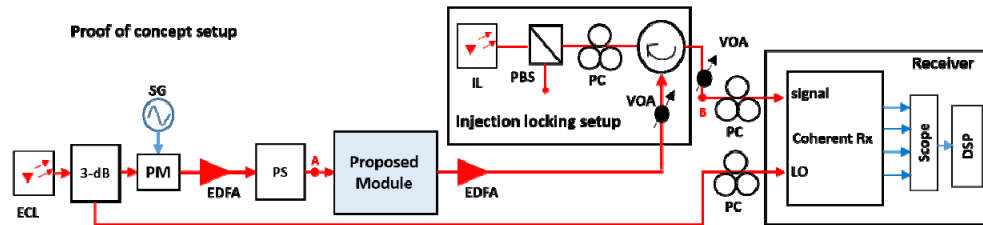


Fig. 3. Experimental setup for proof of concept. ECL: external cavity laser; PS: polarization scrambler; IL: Injection laser; LO: local oscillator laser; Rx: Receiver.

As a proof of concept, we investigate the transfer of a 100-MHz sinusoidal phase modulation through injection locking. Here, a signal generator is used to modulate a CW laser output with an external phase modulator, as shown in Fig. 3. Note that this 100-MHz phase modulation is used to investigate the transfer of phase information through the injection locking process, and is applied externally at the transmitter. As described in the previous section, the polarization-locking module uses 400-kHz phase modulation to reduce polarization fades. The same technique is again used in the experiments described in this section. The polarization of the modulated optical signal was scrambled using a Novoptel EPX1000 polarization scrambler (PS) that allows controlled or random scrambling of the polarization state of the input signal. This scrambling ensured that the proposed module does not cause any suppression of the modulation or unlocking as the polarization state changes. The signal was then passed to the IL setup through the proposed polarization-locking module with an injection ratio of  $-45$  dB ( $-25$  dBm at the input to the slave laser, with a 20-dBm output). The phase modulated signal was then detected by a 25-GHz electrical bandwidth integrated coherent receiver and processed in DSP to recover the peak-to-peak phase swing of the signal.

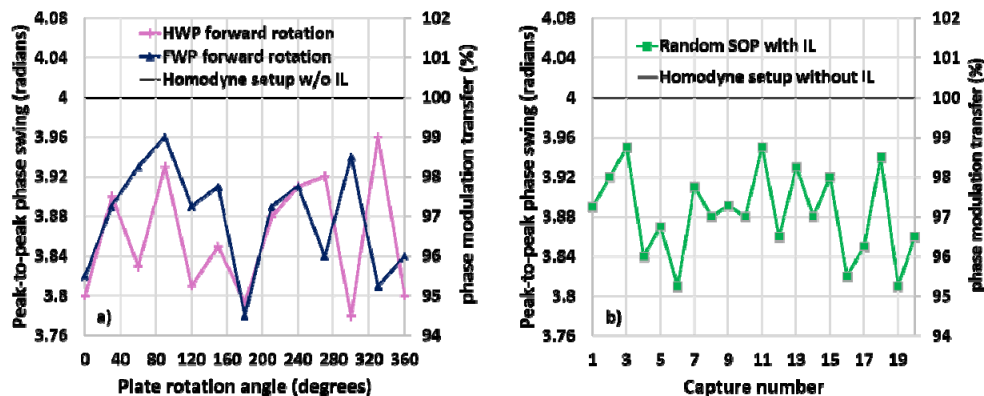


Fig. 4. Peak-to-peak phase swing of the recovered signal and % modulation transfer through IL setup vs.: a) rotation angle of half-wave plate and full-wave plate of the polarization scrambler (PS); b) for 20 data captures each with a random state of polarization (SOP).

In order to ascertain how well phase modulation is transferred through the injection locking stage, we compared the peak-to-peak phase swing of the recovered signal with and without the injection locking stage. For a reference measurement, we passed the signal directly out of the phase modulator (Point A, Fig. 3) to the signal input of the coherent receiver (Point B, Fig. 3). This phase modulator provides a reference swing of 4 radians peak-to-peak ( $= 1.27\pi$  radians). We then compared this with the phase swing when the signal is passed through a polarization scrambler, our polarization-locking module, and the injection

locking stage before the coherent receiver. The reference measurement and the phase swing with the system in place are plotted in Fig. 4, marked on the left vertical axis. The ratio of phase swing measured with this system in place to the reference measurement without gives us a measure of the modulation transfer through our system, plotted on the right vertical axes of Figs. 4(a) and 4(b) as a percentage.

To show that the polarization-locking module makes the injection locking process insensitive to the polarization state of the incoming signal, we first varied the rotation angle of a half-wave plate (HWP) in the PS, then the full-wave plate (FWP), and then both of them simultaneously to cover random points on the Poincaré sphere. Figures 4(a) and 4(b) show that on average, 97% of the input phase swing was transferred (see secondary y-axis) through the IL setup independent of the polarization of the incoming signal (x-axis) with a 2% variation about the average. This indicates that the IL system with the polarization-locking module maintains the lock while transferring phase modulation regardless of the incoming state of polarization.

It is imperative that inclusion of the polarization-locking module in the OIL should not reduce the locking bandwidth, as it may cause loss of lock in the case of low power signals. Thus, the locking bandwidth of the OIL system was investigated with and without the polarization-locking module. The experimental setup is the same as in Fig. 3. The continuous wave ECL output was phase-modulated with a sinusoidal electrical signal whose frequency was swept from 10 MHz to 10 GHz. As the phase modulations are transferred by the OIL within the locking bandwidth, the phase swing of the output of the OIL can help in calculating the locking bandwidth. Figure 5 shows the peak-to-peak swing of the received signal's sinusoidal modulated phase at the output of the OIL setup with and without the polarization-locking module. It is observed that the locking bandwidth does not change with the inclusion of the module. This is an expected result, as the module merely changes the polarization alignment, and so the injection ratio remains the same in both cases, leaving the locking bandwidth unaffected.

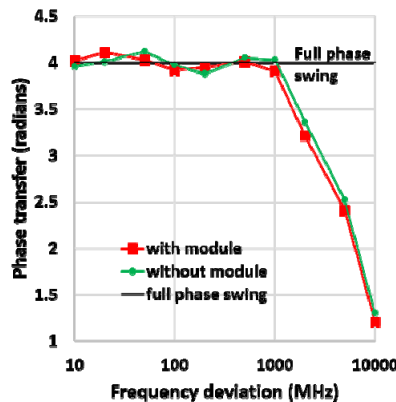


Fig. 5. Phase transfer (radians) vs. frequency deviation (MHz).

#### 4. Back-to-back test with injection locked self-homodyne receiver

The previous section proved that the polarization-locking module allows for phase information to be transferred regardless of the incoming signal's SOP. We now test the performance of this sub-system in a back-to-back setup where injection locking is used to recover the residual carrier from a coherent OFDM signal. The experimental setup consists of a transmitter that modulates a continuous wave (CW) laser output using a complex Mach-Zehnder modulator (CMZM) driven by electrical signals from an arbitrary waveform generator as shown in Fig. 6. A 25-Gbaud QPSK modulated OFDM electrical signal with 100 subcarriers and 156-point FFT length was generated using an arbitrary waveform generator to



drive an optical IQ modulator. A central guard band of 2.5 GHz (10 sub-carriers) was added to keep a clear spectrum containing the optical carrier, preventing transfer of the modulated signal through IL. The amplified signal from the transmitter is noise-loaded using filtered amplified spontaneous emission (ASE) noise from an EDFA covering a 200-GHz bandwidth, which was added to the signal to vary the received OSNR.

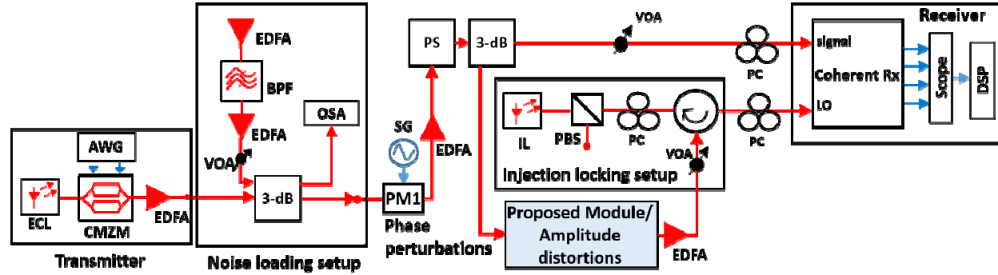


Fig. 6. Experimental setup with proposed polarization-locking module and injection locking setup. CMZM: complex Mach-Zehnder modulator; EDFA: erbium doped fiber amplifier; BPF: bandpass filter; OSA: optical spectrum analyzer; DSP: digital signal processing.

To ensure that the IL replicates the low frequency phase modulations, and that the phase perturbations cancel out in a homodyne receiver setup, the noise-loaded signal was distorted in phase using a phase modulator (PM1 in Fig. 6). For the later part of the experiment, when we used a broad LW laser at the transmitter, the phase modulator was removed. After adding phase perturbations, the polarization of the signal is scrambled using the Novoptel polarization scrambler (PS). The scrambled signal was then split using a 3-dB coupler, where one arm is connected to the polarization-locking module followed by an IL setup and the other arm was directly connected to the signal input of a 25-GHz electrical bandwidth integrated coherent receiver. The outputs of the coherent receiver were connected to a 40-GSa/s 28-GHz bandwidth digital signal oscilloscope (DSO). The data recovery algorithms such as the channel equalization and the residual phase recovery were run as offline DSP.

Figure 7(a) shows performance of injection locking and intradyne systems with or without phase perturbations added to the signal. At lower OSNRs where sufficient errors were measured, the  $Q$ -value calculated from the error vector magnitude ( $Q_{\text{SNR}}$ ) is equal to the  $Q$ -value calculated from the finite BER ( $Q_{\text{BER}}$ ) where  $Q_{\text{BER}}$  for any M-QAM modulation format is [21]

$$Q_{\text{BER}} = 20 \log_{10} \left[ \sqrt{\frac{2(M-1)}{3}} \times \text{erfc}^{-1} \left( \frac{\text{BER} \times \log_2 \sqrt{M}}{\left(1 - \frac{1}{\sqrt{M}}\right)} \right) \right] \quad (5)$$

Figure 7(a) plots the performance versus OSNR for the intradyne system without any added phase perturbations (red dotted line), to provide a reference. When phase perturbations are added at the transmitter, and the receiver is in the intradyne configuration (i.e. without injection locking), the  $Q$  degrades by 5-dB in  $Q$  and an additional 1.5-dB OSNR is required at the 7% hard-decision FEC limit ('error free' BER =  $3.8 \times 10^{-3}$ ). Using the injection locking stage to recover the phase perturbed carrier from the signal compensates the phase fluctuations, as shown in Fig. 7(a) by the match of the curve marked by blue circles with the undistorted intradyne reference (red dots). Moreover, when the polarization of the incoming signal is randomly rotated and using the proposed module for polarization independence (Fig. 7(a), green triangles), the system performance is again the same as the undistorted intradyne reference. To ensure that polarization independent injection locking can also perform without penalty, we include our polarization-locking module, and activated the polarization

scrambler. The performance of this system is plotted as green triangles in Fig. 7(a), and shows a negligible required OSNR penalty at the FEC limit, when compared to the undistorted intradyne reference (red dots). This indicates that the phase fluctuations are sufficiently canceled to be useful for coherent communications systems, even for a random state of polarization of the incoming signal. Moreover, the OIL system provides an additional overall benefit by reducing DSP complexity, because the CFO estimation and compensation algorithms are omitted for OIL.

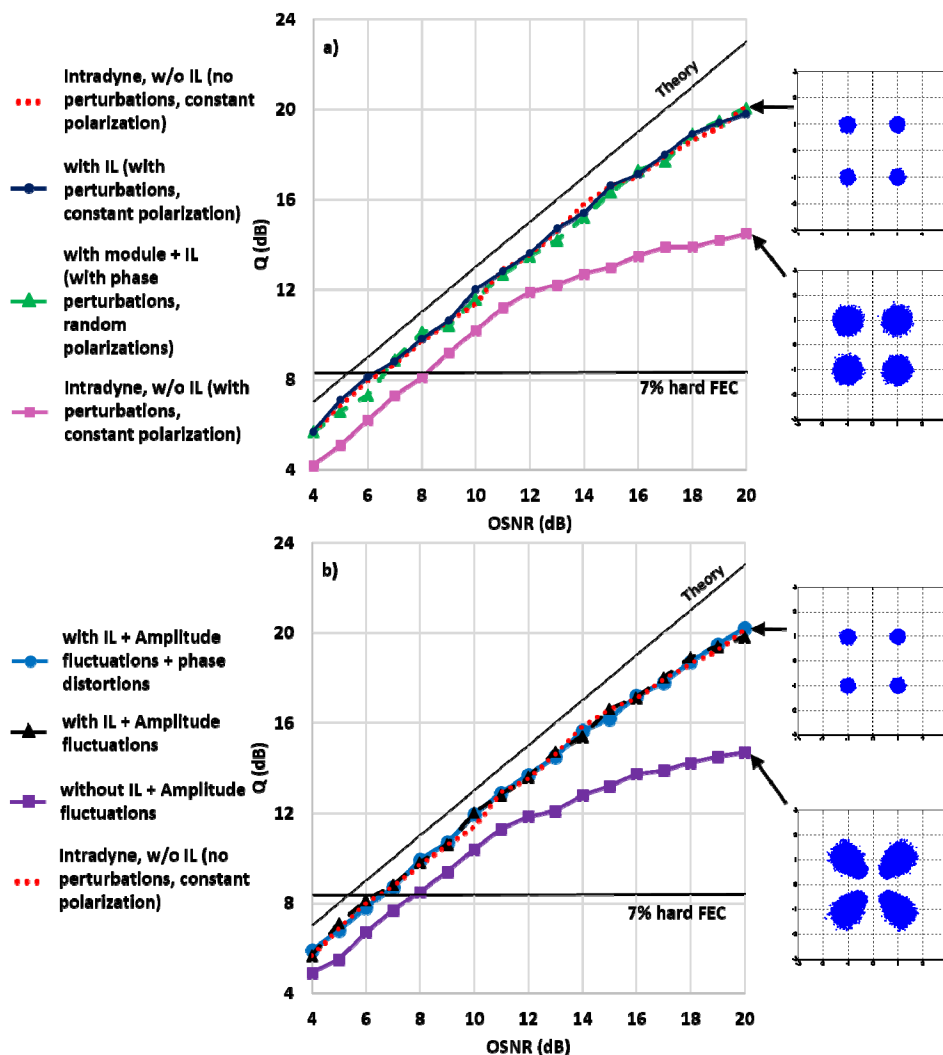


Fig. 7.  $Q$  performance vs. OSNR: a) with or without (w/o) injection locking (IL) in presence of additional phase perturbations; b) with or without (w/o) injection locking (IL) in presence of additional amplitude fluctuations; Insets: Constellations of recovered signals at 22-dB OSNR with and without phase/amplitude perturbations.

The phase perturbations in OFDM systems cause inter-carrier interference (ICI) along with a common phase error (CPE) [22, 23]. The phase error correction algorithms running in the DSP take care of the CPE but cannot completely negate the effects of ICI due to the phase perturbations. Hence, due to ICI and AWGN, the constellations of the recovered signals show circularly symmetric Gaussian spreads of the constellation points, rather than a phase skew as

seen in the inset of Fig. 7(a). With the IL, the system with phase perturbations and constant signal polarization gave similar performance to that of the system without perturbations, confirming that the IL can cancel phase perturbations at the receiver. This is reflected in the inset in Fig. 7(a), where the Gaussian spread of the constellation points is significantly reduced.

As discussed in Section 1, the polarization-locking module may generate amplitude fading in the signal, due to the interference in the 3-dB coupler in the module, which in turn may result in a loss of injected power and thus, the injection lock. Theoretically, these low-frequency amplitude fluctuations are rejected by the IL [19, 20]. To systematically test this, we added additional amplitude fluctuations into our system to verify the AM suppression capabilities of our IL set-up. The amplitude fluctuations were added replacing the polarization-locking module with an intensity modulator driven with a 400-kHz sinusoid.

Figure 7(b) shows that without the locking, compared with intradyne system without perturbations:  $Q$  drops by 5-dB at 20-dB OSNR and the required OSNR at FEC increases by 1.5-dB at hard-FEC limit. When using an injection-locked LO, the system performs similarly to the reference intradyne system. This is because of the inherent rejection of low-frequency amplitude fluctuations through the IL process. Now, with the phase fluctuations turned on and the polarization scrambler also activated, the system again performs similarly to the reference intradyne system without a loss of  $Q$ , confirming the rejection of amplitude fluctuations, the cancellation of phase fluctuations and independence on incoming signal polarization.

## 5. Broad-linewidth laser experiments

The optical injection locking, being able to replicate the carrier phase information up to several GHz, should allow the use of broad LW lasers in coherent communication systems. Relaxing the limit on required LW for coherent systems may lower the cost of coherent transceivers, by allowing a wider range of fabrication tolerances, and operation at lower optical powers. We tested performance in a back-to-back system as in the previous section, here using a broad LW (40 MHz) low-power (0.5 dBm) laser at the transmitter. The phase modulation module was removed from the setup in Fig. 6, as the use of a broad LW laser at the transmitter provides significant phase fluctuations. A 25-Gbaud OFDM signal was again generated with the same OFDM parameters as in previous experiment. The polarization of the injected signal was again scrambled. The system was tested for both QPSK and 16-QAM modulation formats.

A reference  $Q$  curve was plotted over an OSNR sweep using a laser with 100-kHz LW. Its output power was attenuated to 0.5 dBm, to match the output power of the low-performance laser, so that the performance difference between these two systems could be primarily attributed to the difference in laser LWs. The performances with and without the polarization-locking module were similar, as shown in Fig. 8. The  $Q$  of the recovered signal reaches only 16.2 dB for QPSK at 20-dB OSNR even for the 100-kHz LW laser, owing to the OSNR penalty caused by low output power of the laser. The system was then tested using the 40-MHz LW laser. This laser had a 40-MHz LW, despite operating at its specified maximum bias current. This low-performing laser was used in the experiments to test the system under worst-case scenario. Without injection locking, the signal at the receiver was unrecoverable, even when using a spectral peak search for frequency offset compensation and training-aided maximum likelihood phase estimation. With injection locking, signal recovery was possible. Figure 8 shows the measured performance with and without the polarization-locking module in the injection locked setup. For the measurements without polarization locking, the system lost lock when the polarization of the injected signal changed, then required manual adjustment of the polarization controllers to regain the lock. On the other hand, this manual intervention was not needed when the polarization-locking module was used.

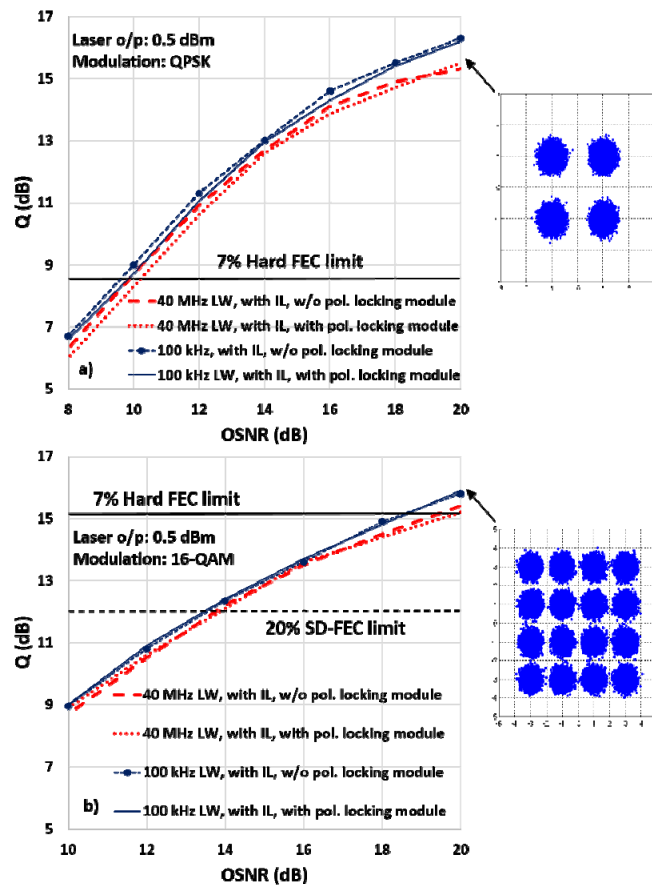


Fig. 8.  $Q$  (dB) vs. OSNR (dB) using a low performance laser (LW = 40 MHz) compared with a standard laser (LW = 100 kHz) for injection locking the local oscillator with and without polarization-locking module for a) QPSK modulation and b) 16-QAM modulation. Insets: Recovered constellations at 22-dB OSNR for QPSK, 16-QAM with LW = 40 MHz.

Comparing the traces for systems using the narrow (100 kHz) and broad (40 MHz) LW lasers at the transmitter, Fig. 8 shows that the IL setup effectively cancels the phase noise due to the broad LW, as the performance was observed to be similar to that of the system using the narrow LW laser. There is a small but measurable required-OSNR penalty of 0.6 dB when using the broad LW laser, compared with the narrow LW laser at the hard FEC limit. A similar performance trend was observed when using 16-QAM modulation where the system using the broad LW laser gives a marginal OSNR penalty of 1.1 dB, compared with that using the narrow LW laser, both at the limit of hard-decision FEC (15.2 dB). Moreover, the performance using the broad LW laser for 16-QAM barely reaches the hard FEC limit at 20-dB OSNR. Nonetheless, soft-decision thresholds can be considered for 16-QAM assuming the use of a concatenated LDPC-convolutional (LDPC-CC(18360,4,24)) code with a 20% overhead [24], giving 'error free' operation for pre-FEC BER of  $2.7 \times 10^{-2}$ . The OSNR penalty reduces to 0.35-dB compared with the narrow LW system at this soft-decision FEC limit. For both the broad and narrow linewidth systems, the polarization locking module was able to maintain the injection lock despite of polarization drifts.

## 6. Field test over a fiber link from Monash Clayton to Caulfield campus

The system was tested over an installed 'field-trial' link from Monash University's Clayton campus to the Caulfield campus. The field link used in this experiment is a 10-km long dedicated 'dark' fiber, resulting in 20-km link transmission with a simple loop-back placed at Caulfield and an overall insertion loss of 5.8 dB (Fig. 9).

The experimental setup is similar to the one shown in Fig. 6. The polarization scrambler and phase modulator are removed from the set-up, as random polarization rotations are provided by the field link and the phase perturbations by the use of the broad LW laser in the transmitter. A signal with same OFDM parameters as in previous back-to-back experiment was transmitted over the field link and received after a single round-trip with an IL-based homodyne receiver setup. Figure 10 shows the  $Q$  of the signal recovered after transmission over the fiber link with and without the polarization-locking module. As expected, the IL system with the module gave similar  $Q$  performance over a wide range of OSNRs, compared with the IL system without the module. This proved that the polarization-locking module did not impart performance penalties to the system. Again, as expected, the IL system without the polarization-locking module lost lock randomly and had to be manually realigned on multiple occasions, whereas the IL with module maintained the lock all through the course of the experiments. The system performances for all cases with the IL cross the forward error correction (FEC) limits, for both the 7% hard-decision FEC for QPSK, and the 20% soft-decision FEC for 16-QAM.



Fig. 9. Map of south-east Melbourne, showing the test link node locations.

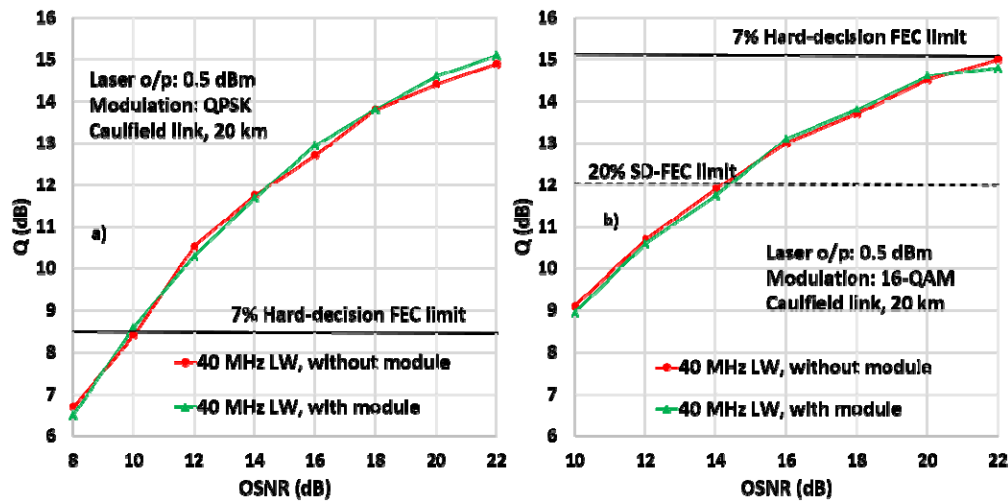


Fig. 10.  $Q$  (dB) vs. OSNR (dB) using low performance laser for a) QPSK modulation and b) 16-QAM modulation format.

From the measurements, we infer the required OSNR is 11 dB for QPSK and 14 dB for 16-QAM, demonstrating that coherent systems, employing our polarization-insensitive IL in installed metropolitan fiber systems, can use lasers with significantly relaxed specifications (e.g. LWs up to 40 MHz, with output powers as low as 0.5-dBm). Critically, the polarization-locking module removes the need for polarization tracking, allowing for operation with an arbitrary input polarization state.

## 7. Conclusions

An optical injection locking (IL) setup is modified with a module that, when added to the IL setup, allows locking independent of the injected signal's polarization. The proposed polarization-locking module enabled the optical injection locking (IL) setup to maintain the lock for all states of polarization of the injected signal without any considerable loss in the  $Q$  performance. The system was also tested over a 20-km field link, using a 40-MHz LW 0.5-dBm transmitter laser. The random fluctuations in the polarization of the signal due to random events in the surroundings of the link was taken care of by the proposed polarization-locking module. The resulting continuously-locked IL setup cancelled the phase noise effects of the broad LW laser. Thus, the complete setup with the polarization-locking module along with the IL relaxed the constraints on the laser specifications and proved to be capable for practical implementation, which was difficult until now due to the polarization-sensitivity of IL's locking mechanism.

## Funding

Australian Research Council's (ARC) Centre of Excellence Laureate Fellowship schemes (CE110001018, FL130100041).

## Acknowledgement

We thank VPIphotonics ([www.vpiphotonics.com](http://www.vpiphotonics.com)) for their support under the university program.